Crystal Lattice Dynamics of the Substitutional Solid Solutions in the Bi(Gd) - Fe - O and Bi(Nd) - Fe - O Systems

Valery Sobol[1], Barys Korzun[2], Cheslav Fedorcov[1], Olga Mazurenko[3], Temirkhan Bizhigitov[4], Sabit Tomaev[4], Bibara Nushnimbaeva[4], Sofia Egemberdieva[4], Altynbek Nauryzbaev[4]

[1]Belarusian State Pedagogical University, 18 Sovetskaya St., Minsk 220030, Belarus

[2]The City University of New York, Borough of Manhattan Community College, 199 Chambers St., New York, NY 10007, U.S.A.

[3]Belarusian Republican Foundation for Fundamental Research, 66 Nezavisimosti Ave., Minsk 220072, Belarus

[4]Taraz State Pedagogical University, 62 Tole bi St., Taraz 080001, Kazakhstan

ABSTRACT

The substitutional solid solutions in the Bi(Gd) - Fe - O and Bi(Nd) - Fe - O systems of the $Bi_{1-x}Gd_xFeO_3$ and $Bi_{1-x}Nd_xFeO_3$ types with x up to 0.20 were synthesized by the solid-state reaction method and investigated using X-ray diffraction analysis and infrared reflective spectrometry in the wavelength range from 12.5 to 24 μm. It was determined that the $Bi_{1-x}Gd_xFeO_3$ and $Bi_{1-x}Nd_xFeO_3$ crystal structure is a distorted form of perovskite, R3c space group. Two extremums at 18.2 μm (strong extremum) and 22.5 μm (rather weak extremum) on the infrared reflection spectra of the $Bi_{1-x}Gd_xFeO_3$ and $Bi_{1-x}Nd_xFeO_3$ solid solutions were discovered. The extremum at 18.2 μm corresponds to the Fe – O stretching vibrations and the extremum at 22.5 μm corresponds to the O - Fe – O bending vibrations of the FeO_6 groups. The growth of reflectivity of the $Bi_{1-x}Gd_xFeO_3$ and $Bi_{1-x}Nd_xFeO_3$ solid solutions in comparison with pure $BiFeO_3$ and the displacement of the reflectivity band maximum into the side of the spectrum with longer wavelengths with the increase of the atomic part of the substitutive element x up to 0.20 were found.

INTRODUCTION

Bismuth ferrite $BiFeO_3$ is a promising magnetoelectric material due to the coexistence of both ferroelectric and antiferromagnetic orders in this material at room temperature [1]. The observed switching of antiferromagnetic domain in the films of $BiFeO_3$ by the external electric field indicates that there is a possibility of applying this material in novel electronic devices. It is desirable to transform the antiferromagnetic spin configuration of $BiFeO_3$ into the ferromagnetic one by an action on the spiral modulated spin structure. Chemical doping can modify both the electric conductivity and the spiral spin structure to intensify the macroscopic properties. In particular, the use of rare-earth elements Gd and Nd for the substitution of Bi has been proposed [2, 3]. The effect of the substitution of Bi by Gd on the structural, magnetic, and dielectric properties was studied in [4, 5]. Electron spin resonance and magnetic properties of Gd-substituted $BiFeO_3$ ceramics were studied in [6]. The crystal structure, magnetic properties, and complex impedance spectroscopy of the Nd-doped $BiFeO_3$ materials were investigated by X-ray diffraction, Raman scattering, vibrating sample magnetometer, and complex impedance spectroscopy [7]. Crystal structure refinement of the $Bi_{1-x}Nd_xFeO_3$ multiferroic by the Rietveld method was performed in [8]. The magnetic susceptibility, thermal expansion, electrical conductivity, and thermo-EMF of $Bi_{0.85}Nd_{0.15}FeO_3$ were studied [9].

The crystal lattice dynamics of $BiFeO_3$ was studied in papers [10 – 12]. It has been reported that $BiFeO_3$ with a distorted rhombohedral structure, *R3c* space group, yields 18 optical phonon modes among which 13 are Raman active modes. Reflectivity of the multiferroic $BiFeO_3$ ceramics in the wavenumber range from 20 to 800 cm^{-1} was investigated at 20, 300, 650, and 950 K [10]. IR reflection and transmission spectra of the $BiFeO_3$ ceramic samples were measured in the wavenumber range from 5 to 1000 cm^{-1} in the temperature interval 10 – 500 K [11]. Two strong absorptive bands at about 560 and 440 cm^{-1} in the FT-IR spectrum were found for the $BiFeO_3$ nanopowder prepared by the sucrose-assisted combustion method [12]. Information about the influence of the Gd and Nd substitution on the crystal lattice dynamics of the doped $BiFeO_3$ materials is rather scarce. Raman spectroscopy of Gd- and Nd-substituted $BiFeO_3$ ceramics in the interval from 100 to 800 cm^{-1} discovered 12 Raman active modes [6, 8].

The goal of this paper is to prepare the substitutional solid solutions in the Bi(Gd) - Fe - O and Bi(Nd) - Fe - O systems to determine the influence of the substitution of Bi by Gd and Nd on the crystal lattice dynamics in the range from 12.5 to 24 μm.

EXPERIMENTAL DETAILS

The substitutional solid solutions in the Bi(Gd) - Fe - O and Bi(Nd) - Fe - O systems of the types $Bi_{1-x}Nd_xFeO_3$ and $Bi_{1-x}Gd_xFeO_3$ with the atomic part of the substitutive element x equal up to 0.20 were synthesized by the solid-state reaction method using powders of oxides Bi_2O_3, Fe_2O_3, and Gd_2O_3, or Nd_2O_3 of pure grade quality. The X-ray diffraction method was applied using the diffractometer Dron-3 on monochromatic Cu K_α-radiation (1.5406 Å). The experimental data were collected during scanning repeated ten times in the 2Θ range from 20° to 80° at the scanning rate of 10°/6 min. The infrared reflection spectra of the samples in tablet powder mixtures were recorded with VERTEX 80v FT-IR spectrometer (Bruker) in the range from 12.5 μm (800 cm^{-1}) to 24 μm (416 cm^{-1}). As standards for the recording of the absolute values of the reflection coefficient R, an aluminium mirror with R = 97% and a single crystal silicon wafer were used.

DISCUSSION

X-ray powder diffraction

X-ray diffraction patterns for the $Bi_{1-x}Gd_xFeO_3$ solid solutions with molar parts of $GdFeO_3$ corresponding to x = 0.05, 0.10, 0.15, and 0.20 are presented on Figure 1, and X-ray diffraction patterns for the $Bi_{1-x}Nd_xFeO_3$ solid solutions with molar parts of $NdFeO_3$ corresponding to x = 0.05, 0.10, 0.15, and 0.20 are presented on Figure 2. It was found that the crystal structure for both the $Bi_{1-x}Gd_xFeO_3$ and $Bi_{1-x}Nd_xFeO_3$ solid solutions is the rhombohedrally distorted structure of perovskite, *R3c* space group. There is a shift of X-ray reflexes that clearly shows the formation of solid solutions in the $BiFeO_3 - GdFeO_3$ and $BiFeO_3 - NdFeO_3$ systems.
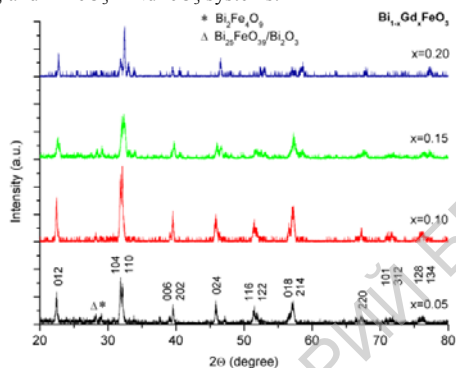

Figure 1. X-ray diffraction patterns for the $Bi_{1-x}Gd_xFeO_3$ solid solutions with molar parts of $GdFeO_3$ corresponding to x = 0.05, 0.10, 0.15, and 0.20

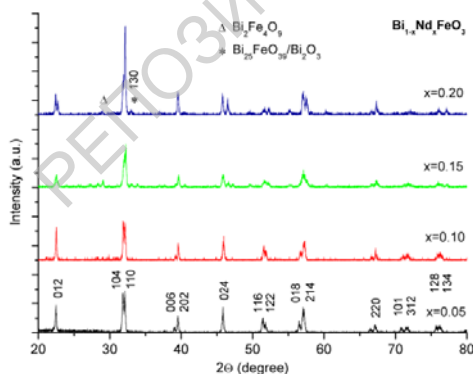**Figure 2.** X-ray diffraction patterns for the $Bi_{1-x}Nd_xFeO_3$ solid solutions with molar parts of $NdFeO_3$ corresponding to x = 0.05, 0.10, 0.15, and 0.20

Additional reflexes are detected for solid solutions of both series. These reflexes can be attributed to the phases which are based on ternary compounds $Bi_{25}FeO_{39}$ and $Bi_2Fe_4O_9$ formed in the $Bi_2O_3 - Fe_2O_3$ quasibinary system for the molar ratio of

Bi_2O_3 and Fe_2O_3 being 25:1 and 1:2, respectively. The amount of the impurity phases is larger for the Bi(Gd) - Fe - O system and can reach 10 molar %.

$BiFeO_3$ exists in the $Bi_2O_3 - Fe_2O_3$ quasibinary system for the molar ratio of Bi_2O_3 and Fe_2O_3 being 1:1 [13, 14]. Its melting occurs in accordance with the peritectoid reaction. This means that this compound in principle cannot be prepared by preparation methods from the melt. Additionally, the high volatility of bismuth oxide Bi_2O_3 has to be taken into account. All of this leads to a thermodynamic instability of $BiFeO_3$ and impossibility to synthesize single-phase $BiFeO_3$ by the solid-state reaction. Synthesis in accordance with the ceramic technology produces the pseudomonophasic composition with accuracy of up to 3% by weight of impurity of $Bi_{25}FeO_{39}$ [11].

It should be noted that the presence of impurity phases affects physical properties and partially changes quantitative values. Nevertheless, the impurity phases cannot be the cause of the observed phenomena since their content is relatively small to sufficiently affect physical properties of the $Bi_{1-x}Gd_xFeO_3$ and $Bi_{1-x}Nd_xFeO_3$ solid solutions.

Infrared Reflection

IR reflection spectra of the $Bi_{1-x}Gd_xFeO_3$ and $Bi_{1-x}Nd_xFeO_3$ solid solutions (Figures 3 and 4) show the activation of the strength of the optical oscillator when an insignificant change in the concentration of doping elements takes place. When the reflection at 18 μm is increased, the position of the band's extremum shifts toward the longer wavelengths.
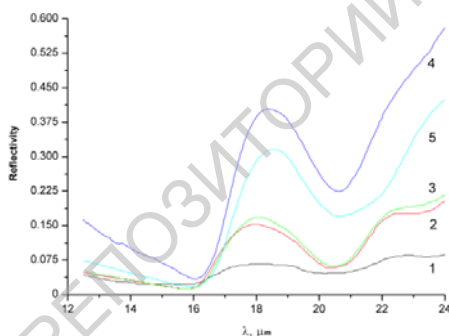

Figure 3. IR reflection spectra of $BiFeO_3$ and the $Bi_{1-x}Gd_xFeO_3$ solid solutions at room temperature (1 – $BiFeO_3$; 2 – $Bi_{0.95}Gd_{0.05}FeO_3$, 3 – $Bi_{0.90}Gd_{0.10}FeO_3$; 4 – $Bi_{0.85}Gd_{0.15}FeO_3$; 5 – $Bi_{0.80}Gd_{0.20}FeO_3$)

According to the results of [11], an extremum at 18 μm in undoped $BiFeO_3$ is also observed, but it is sufficiently appreciable in magnitude (about 20%) at liquid hydrogen temperature and, as the temperature increases, decreases and also weakly shifts toward the longer wavelengths. In the present study, an opposite behaviour is observed. The reflection in the region of 18 μm is initially small in comparison with the results of [10]. When the content of the substitutive chemical elements increases, the reflection also increases and reaches about 0.40 upon the substitution of atomic part of 0.20.

An increase in reflection with a decrease in temperature was reported for pure $BiFeO_3$ [11], where the reflection coefficient is 0.37 and 0.50 for 295 K and 50 K, respectively. It can be concluded that both the decrease in the intensity of vibrations with

a decreased temperature and the incorporation of the substitutive atoms of Gd and Nd into the Bi-sublattice lead to a similar effect of activation of oscillations.
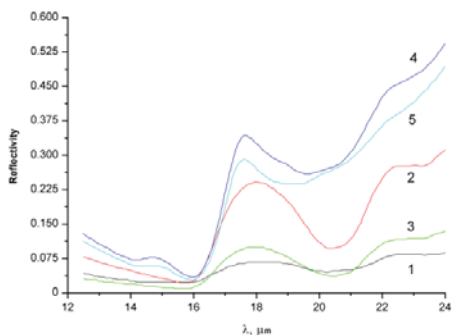

Figure 4. IR reflection spectra of $BiFeO_3$ and the $Bi_{1-x}Nd_xFeO_3$ solid solutions at room temperature (1 – $BiFeO_3$; 2 – $Bi_{0.95}Nd_{0.05}FeO_3$, 3 – $Bi_{0.90}Nd_{0.10}FeO_3$; 4 – $Bi_{0.85}Nd_{0.15}FeO_3$; 5 – $Bi_{0.80}Nd_{0.20}FeO_3$)

Crystal Structure and Vibrational Modes

Eight Bi atoms form a rhombohedron elongated along the spatial diagonal having one Bi atom in the centre of the unit cell of $BiFeO_3$ (Figure 5).
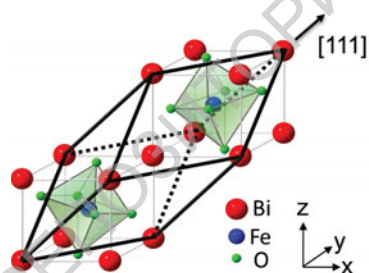

Figure 5. The forming of elementary cell of distorted rhombohedrally perovskite structure for $BiFeO_3$

According to the group theory analysis and first-principles calculation, $BiFeO_3$ can be classified as a highly distorted rhombohedrally perovskite with *R3c* space group, which is expected to have 13 ($4A_1 + 9E$) Raman active modes [15], where A_1 modes are polarized along the z-axis and E modes are polarized in the x-y plane. It is asserted that the E(8) mode at 433 cm^{-1} (23.1 µm) detected in single crystal of $BiFeO_3$ should be dominated by oxygen motion [16]. The nature of the two strong reflection bands in perovskite $BiFeO_3$ at 18.2 µm (550 cm^{-1}) and 22.5 µm (445 cm^{-1}) was attributed to the Fe-O stretching and the O–Fe–O bending vibrations of the FeO_6 groups in perovskite $BiFeO_3$, respectively [12, 17]. The same nature, namely the Fe-O stretching and the O–Fe–O bending vibrations of the FeO_6 groups should be attributed to the corresponding reflection bands of the $Bi_{1-x}Gd_xFeO_3$ and $Bi_{1-x}Nd_xFeO_3$ solid solutions. The influence of the Ga and Nd substitution on the oxygen ions in the FeO_6 group through the valence

3247

chains containing ions –Bi–O–Gd(Nd)–O–Bi– should be also taken into account. The increase in reflection and the displacement of the resonant wavelength with the substitution of Bi by Gd or Nd can be explained by the decrease of the reduced mass of the chain of valence bonds. In the approximation of elastic interactions, the change $\Delta\lambda$ of the resonant wavelength λ can be approximately evaluated by the expression $(\Delta\lambda/\lambda) \infty$ $(\Delta m/2m)$, where m is the mass of the resonant ions and Δm is the change of the mass of the resonant ions occurring with the substitution of Bi by Gd and Nd.

SUMMARY

Two extremums at 18.2 μm (strong extremum) and 22.5 μm (rather weak extremum) on the infrared reflection spectra of the $Bi_{1-x}Gd_xFeO_3$ and $Bi_{1-x}Nd_xFeO_3$ solid solutions were discovered. The extremum at 18.2 μm corresponds to the Fe–O stretching vibrations and the extremum at 22.5 μm corresponds to the O–Fe–O bending vibrations of the FeO_6 groups. The increase of the atomic part of the substitutive element x up to 0.20 leads to the growth of reflectivity and the absorption coefficients of the $Bi_{1-x}Gd_xFeO_3$ and $Bi_{1-x}Nd_xFeO_3$ solid solutions in comparison with $BiFeO_3$. The displacement of the reflectivity band maximum into the side of the spectrum with longer wavelengths with the increase of the content of the substitutive elements was also found. Such behavior of the spectra can be explained by the decreasing elastic constants of the $Bi_{1-x}Gd_xFeO_3$ and $Bi_{1-x}Nd_xFeO_3$ solid solutions occurring when the new substitution-induced bonds Gd–O and Nd–O are formed.

References

1. S.M. Skinner, IEEE Trans. Parts Mater. Packaging **6**, 68 (1970).
2. Y.E. Roginskaya, Y.N. Venevtsev, S.A. Fedulov, G.S. Zhdanov, Kristallografiya **8**, 1224 (1965) [Sov. Phys. Crystallogr. **8**, 490 (1964)].
3. M. Polomska, W. Kaczmarek, Z. Pajak, Phys. Status Solidi A, **23**, 567 (1974).
4. J.-B. Li, G.H. Rao, Y. Xiao, J.K. Liang, J. Luo, G.Y. Liu, J.R. Chen, Acta Materialia **58** (10), 3701 (2010).
5. V.V. Lazenka, G. Zhang, J. Vanacken, I.I. Makoed, A.F. Ravinski, V.V. Moshchalkov, Journal of Physics D: Applied Physics, **45** (12), 125002 (2012).
6. M. Kumar, P.C. Sati, S. Chhoker, V. Sajal, Ceramics International **41**, 777 (2015).
7. D.V. Thang, D.T.X. Thao, N.V. Minh, Journal of Magnetics **21** (1), 29 (2016).
8. A. Kumar, D. Varshney, Ceramics International **38**, 3935 (2012).
9. A. Klyndyuk, Y. Chizhova, Universal Journal of Materials Science **3** (1), 6 (2015).
10. S. Kamba, D. Nuzhnyy, M. Savinov, J. Šebek, J. Petzelt, J. Prokleška, R. Haumont, and J. Kreisel, Phys. Rev. B **75**, 024403 (2007).
11. G.A. Komandin, V.I. Torgashev, A.A. Volkov, O.E. Porodinkov, Fiz. Tv. Tela, **52** (4), 684 (2010).
12. S. Farhadi, M. Zaidi, Journal of Molecular Catalysis A: Chemical **299**, 18 (2009).
13. H. Koizumi, N. Nirizaki, T. Ikeda, Jpn. Appl. Phys. **3**, 495 (1964).
14. E.I. Speranskaya, V.M. Skorikov, E.Y. Rode, V.A. Terehova, Izv. AN SSSR. Ser. Chimicheskaya 5, 905 (1965).
15. H. Wu, Y.B. Lin, J.J. Gong, F. Zhang, M. Zeng, M.H. Qin, Z. Zhang, Q. Ru, Z.W. Liu, X.S. Gao, J.M. Liu, J. Phys. D Appl. Phys. **46**, 145001 (2013).
16. R.P.S.M. Lobo, R.L. Moreira, D. Lebeugle, D. Colson, Phys. Rev. B **76**, 172105 (2007).
17. K. Nakamoto, Infrared and Raman Spectra of Inorganic and Coordination Compounds, Fourth ed., Wiley, New York, 1986.